EUROPEAN ORGANIZATION FOR NUCLEAR RESEARCH
CERN – SPS DIVISION

CERN SPS/86 – 21(MS)

COMPUTER CALCULATION OF THE LONGITUDINAL IMPEDANCE OF CYLINDRICALLY SYMMETRIC STRUCTURES AND ITS APPLICATION TO THE SPS

L.Vos

Abstract

A new program which calculates the longitudinal impedance of cylindrical vacuum chambers is presented.It is used to analyse bellows and to find a physical explanation for the impedance of these structures.The impedance of the SPS vacuum chamber is calculated with the program and then compared with the impedance values obtained with beam measurements of various types.The agreement is very good for the inductive impedance.Beam measurements of the shunt impedance suggest a broadband model with a quality factor of 6 which is in reasonable agreement with the up to now accepted $Q = 1$ resonator.

Prévessin – August 1986

CONTENTS

TABLES

REFERENCES

[1] T.Weiland Transverse beam cavity interaction DESY 82-015 March 1982
[2] H.Hereward Coupling impedance of a cross-section change for high frequencies CERN/ISR-DI/75-47 October 1975
[3] D.Boussard,J.Gareyte Measurements of the SPS coupling impedance Improvement Report 181 June 1980
[4] L.Evans,J.Gareyte Performance Limitations of the CERN SPS Collider CERN SPS/85-19 May 1985
[5] V.I.Balbekov et al Measurement of charateristics of longitudinal microwave beam instability in the IHEP proton synchrotron Serpukhov 1985
[6] V.I.Balbekov Preprint 85-128 (in Russian) Serpukhov 1985
[7] D.Boussard;CERN Report Lab II/RF/int./75-2 1975
[8] A.Hofmann;Single beam collective phenomena – Longitudinal CERN 77-13 19 July 1977

1. INTRODUCTION

The impedance of an accelerator as seen by the beam is one of the major parameters which determine the performance of a machine.It is in general sufficient to quote the longitudinal value of the impedance from which the transverse value can easily be derived.This report deals with impedances at relatively high frequencies,that is frequencies for which the skin effect is dominated by the impedance caused by cross section variations of the vacuum chamber.In a machine like the SPS many of the vacuum chamber volumes are cylindrically symmetric,or can be conveniently approximated by cylindrical structures.A future machine as the LHC will be completely cylindrical with a few minor exceptions.Hence it is justified to concentrate the calculations on these kind of structures.While this simplifies considerably the task of calculating a global impedance we are still faced with an impressive amount of complexity in a machine like the SPS. Indeed the SPS contains very regular structures like bellows as well as a sequence of cylinders with various radii.In principle the response of these structures can be calculated using programs which give the answers in the time domain [1]. However it is not possible to probe the frequency domain to sufficiently high frequencies and the output needs further treatment to obtain a value of the impedance.Moreover the interpretation of some of the results obtained with these kind of programs was less than obvious,at least for the author. Therefore we embarked on the task of writing a program which calculates the longitudinal impedance for an arbitrary sequence of cylindrical crosssection variations and which is the subject of this paper. The principle of the calculation is given in the next paragraph followed by the theoretical development.The paper then proceeds with results obtained with bellows and some conclusions that can be drawn at that stage.The first part ends with the calculation of some arbitrary structures.In the second part the impedance calculated from the SPS hardware is compared with the values obtained with beam measurements.Although our main interest lies with the SPS a glance is taken at the impedance of the Serpukhov machine which has very interesting characteristics.

2. PRINCIPLE OF THE COMPUTATION

The recipe of the computation has been given in the paper by H.Hereward in 1975 [2] The procedure is as follows:

The wave equations are written down for a smooth cylindrical pipe.The radial boundary conditions generate spatial modes. Their number is theoretically infinite,but in practice good solutions can be found with a very limited number as will be shown later. Next a radial discontinuity is introduced which generates waves that obey continuity equations in the longitudinal direction.These equations can be manipulated into a set of linear equations so that all the field coefficients can be determined. The derivation of the longitudinal impedance $Z_{\parallel}$ is straightforward.

3. THEORETICAL DEVELOPMENT OF THE EQUATIONS

The coordinate system is shown in fig 1.

3.1 Smooth wall case

A charge is travelling down the center line of the pipe according to a $e^{j\omega t-\gamma s}$ propagation law.Symmetry imposes solutions which belong to the TM wave family.Hence only the components H_{ϕ}, E_r and E_s will be different from zero.Furthermore,all the derivatives with respect to ϕ will be zero due to the symmetry in ϕ. Maxwell's equations can now be written down in the required detail. The vector form of the equations is :

$$\mathrm{rot}\,\bar{E} = -\mu(\delta\bar{H}/\delta t)$$

$$\mathrm{rot}\,\bar{H} = \varepsilon_0(\delta\bar{E}/\delta t)$$

With the preceding simplifications this leads to

$$\begin{aligned} \gamma E_r + (\delta E_s/\delta r) &= j\omega\mu H_\phi \\ \gamma H_\phi &= j\omega\varepsilon_0 E_r \\ (\delta r H_\phi/\delta r)/r &= j\omega\varepsilon_0 E_s \end{aligned} \tag{1}$$

These equations can be solved for H_ϕ which gives the following differential equation of second order:

$$\frac{\delta^2 H_\phi}{\delta r^2} + \frac{\delta H_\phi}{r\delta r} + (\gamma^2+k^2)H_\phi(1-\frac{1}{r^2(\gamma^2+k^2)}) = 0 \tag{2}$$

Here the following substitution is used : $k=\omega/c$,where ω is the angular frequency and c the speed of-light.The previous equation can be transformed in the well known "Bessel" differential equation.

$$\frac{\delta^2 H_\phi}{\delta r^2(\gamma^2+k^2)} + \frac{1}{r\sqrt{(\gamma^2+k^2)}}\frac{\delta H_\phi}{\delta r\sqrt{(\gamma^2+k^2)}} + H_\phi(1-\frac{1}{r^2(\gamma^2+k^2)}) = 0 \tag{3}$$

Mathematically the whole family of Bessel functions are possible solutions. The Bessel function of the first kind is choosen since it ensures finite solutions in the center of the pipe. The set of equations (1) and the Bessel equation (3) yield together the following solution :

$$\begin{aligned} H_\phi &= A_H J_1[r\sqrt{(\gamma^2+k^2)}] \\ E_s &= (A_H/j\omega\varepsilon_0)\sqrt{(\gamma^2+k^2)}J_0[r(\gamma^2+k^2)] \\ E_r &= (\gamma A_H/j\omega\varepsilon_0)J_1[r(\gamma^2+k^2)] \end{aligned} \tag{4}$$

The integration constant A_H can be found from the boundary conditions.When the pipe material has infinite conductivity,or in practice sufficiently high conductivity,then $E_s=0$ at the inner pipe surface $r=a$.Hence γ will take values such that $J_0[a(\gamma^2+k^2)]=0$. Or differently:

$$a\sqrt{(\gamma^2{}_m+k^2)} = z_m$$

where z_m is the m^{th} zero of J_0

. Some normalisations can be introduced. The pipe radius **a** is used as a normalisation coefficient.This leads to the following new geometric variables:

$$p = r/\mathbf{a}$$
$$u = s/\mathbf{a}$$

The normalized angular frequency becomes:

$$W = \omega/cz_1/\mathbf{a}$$

Also the propagation factors change since

$$r\sqrt{(\gamma^2+k^2)} = p\sqrt{(\Gamma_m{}^2+k_n{}^2)} = pz_m$$

with

$$k_n = a\,k$$
$$\Gamma_m = a\,\gamma$$

The solutions for the three fields can be written for every possible propagation constant Γ_m:

$$B_{\phi m} = j\mu A_m J_1(pz_m)e^{j\omega t - \Gamma_m u}$$

$$E_{sm} = \sqrt{(\mu/\varepsilon_0)}(z_m/k_n)A_m J_0(pz_m)e^{j\omega t - \Gamma_m u} \tag{5}$$

$$E_{rm} = \sqrt{(\mu/\varepsilon_0)}(\Gamma_m/k_n)A_m J_1(pz_m)e^{j\omega t - \Gamma_m u}$$

The preceding equations are valid for propagation in the positive u direction. For an excitation of the system in the opposite direction simply replace Γ_m by $-\Gamma_m$
A final remark on the Bessel functions which describe the spatial distribution of the fields.The function J_0 is a 'cos'like function while J_1 is a 'sin'like function.Indeed for a set-up of parallel plates very similar solutions are found but with spatial sin and cos functions

3.2 Cylindrical pipe with discontinuity

The system is shown in figure 2

A charge ρ is travelling from left to right.

$$\rho = \hat{\rho}e^{j(\omega t - k_n u/\beta)}$$

β = speed of the charge v/speed of light c

In the general case a wave F is travelling in the forward direction,i.e. the direction of the moving charge, and a wave B in the backward direction starting from the discontinuity.The origin of these waves can be understood from the requirement of field continuity.Indeed,the space charge is perfectly continous at the step for $0<p<1$ but has to be balanced by the F-wave for $1<p<P$.(There is no space charge to the left of the step for $1<p<P$!) The link between space charge and field is given by Ampère's or Gauss' law.Using the last one gives:

$2\pi r E_{r\,sc} = \rho/\varepsilon_0$ $\qquad$ $E_{r\,sc}$ is the space charge field

$$E_{r\,sc} = (\rho/2\pi\varepsilon_0 a)/p$$

For $1<p<P$ $\quad E_r + E_{r\,sc} = 0$ at the right hand side of the step.
The continuity equations between the F-wave and B-wave can be written.The integration constants A_m are replaced by F_m and B_m respectively.This yields the following set of equations

$$\begin{array}{lll} \rho c k_n/2\pi a p & = -\Sigma_m \Gamma_{Pm} J_1 F_m & (E_r \quad 1<p<P) \\ \Sigma_m \Gamma_m J_1 B_m = & -\Sigma_m \Gamma_{Pm} J_1 F_m & (E_r \quad p<1) \\ \Sigma_m z_m J_0 B_m & = \Sigma_m z_{Pm} J_0 F_m & (E_s \quad p<1) \\ \Sigma_m J_1 B_m & = \Sigma_m J_1 F_m & (H_\phi \quad p<1) \end{array} \tag{6}$$

The factors z_{Pm} and Γ_{Pm} are respectively the zero's of the Bessel functions and the corresponding propagation constant in the pipe with normal radius P. Note that the last two equations are redundant.
Our aim is now to find values for the constants F_m and B_m.Remark that the equations contain an infinite sum in m. In fact it ressembles very much a Fourier analysis if only the J_0 and J_1 were cos and sin !The Bessel functions have similar orthogonal properties as the cos and sin functions which allow a Fourier type of analysis of the infinite sums. As an example take one of the equations of the set:

$$\Sigma_m J_1 B_m \qquad = \Sigma_m J_1 F_m$$

Multiply both sides with $pJ_1(z_n p)$ and integrate over p from 0 to 1. This operation singles out a particular mode n :

$$B_n = \frac{2}{J_1(z_n)} \Sigma_m \frac{z_{Pm}}{z_n{}^2 - z_{Pm}{}^2} \quad J_0(z_{Pm})F_m \tag{7}$$

The same technique can be applied to the first equation of the set (6) which describes the continuity between field and space charge.

$$F_n = \frac{-2J_0(z_{Pn})z_{Pn}}{P^2\Gamma_n{}^P J_1{}^2(z_n)} \Sigma_m \frac{\Gamma_m J_1(z_m)}{z_m{}^2 - z_{Pn}{}^2} B_m - \frac{\rho c k_n J_0(z_{Pn})}{\pi a \Gamma_n{}^P P^2 J_1{}^2(z_n) z_{Pn}} \tag{8}$$

The quantities B_n can be considered as components of a vector B.The same is true for F_n and F.Hence equations (7) and (8) can be written more elegantly in matrix form where the substitutions are obvious:

$$\begin{aligned} B \quad - T_1.F \quad &= 0 \\ T_2.B \quad + \quad F \quad &= -C \end{aligned} \tag{9}$$

The square matrices T_1 and T_2 can be completely determined from the geometry.The column matrix C is determined by the passing charge.

3.3 Extension to double step

The set-up is shown in figure 3.

Waves are generated at the two steps when an electric charge passes through the pipe.At each step the continuity equations can be written down as was done for a single discontinuity.Proceding along the same lines the following set of matrix equations is obtained :

$$\begin{aligned} B_1 \quad - \quad T_1.F_1 \quad - T_1.AT.B_2 \qquad\qquad &= 0 \\ T_2.B_1 \quad + \quad F_1 \quad - \quad AT.B_2 \qquad\qquad &= -Ce^{jk_n u_1}/\beta \\ - \quad AT.F_1 \quad + \quad B_2 \quad + T_2.F_2 \quad &= Ce^{jk_n u_2}/\beta \\ -AT.T_1.F_1 \quad - \quad T_1.B_2 \quad + \quad F_2 \quad &= 0 \end{aligned} \tag{10}$$

The matrices T_1 and T_2 are exactly the same as before.The new matrix AT is a diagonal matrix.Examine the continuity of the first step.The waves B_1 and F_1 participate directly in the equation while B_2 first propagates from u_2 to u_1.This feature is taken care off by AT.Its diagonal elements are:

$$AT(m,m) = e^{-\Gamma_{Pm}(u_2-u_1)}$$

The exponential factor of the C-term on the right comes about from the same reasons.
The previous calculation makes it possible to compute a single bellows convolution or an open-ended cavity.However,bellows are very rarely made up of one convolution only and important vacuum chamber sections in the SPS are much more complicated than that.Therefore our goal will be slightly more ambitious.To explain the procedure turn back to a single discontinuity but use the symbols of figure 3.The main difference is that the normalising dimension a is not necessarily a pipe dimension. The quantities P_1,Γ_1,Z_1 are the normalised values for the radius, the propagation and the zero of J_0 at the left of the discontinuity. The quantities to the right carry the index $_2$.
The matrix elements of T_1,T_2 and C can be written down. The calculation is of course identical as before.

$$T_1(n,m) = \frac{2z_{2m}J_0(z_{2m}P_1)}{(z_{1n}^2-z_{2m}^2)J_1[z_n]P_1}$$

$$T_2(n,m) = \frac{2\Gamma_{1m}z_{2Pn}P_1J_0[z_{2Pn}P_1]J_1[z_m]}{(z_{1m}^2-z_{2Pn}^2)\Gamma_{2n}J_1^2[z_n]P_2^2} \qquad (11)$$

$$C(n) = (\rho c/a)\frac{k_nJ_0[z_{2Pn}P_1]}{\pi P_2z_n\Gamma_{2n}J_1^2[z_n]P_2^2}$$

Extending the method to structures with 2 discontinuities as shown in fig 4 similar equations are obtained as for the longitudinally symmetric cavity of fig 3.The first two lines of the matrix equation refer to the first discontinuity,the following two lines to the second discontinuity.It is easy to construct the relevant matrices T_1 ,T_2,an C.They are as given in (11) where index $_1$ refers to quantities to the left of the step and $_2$ to quantities to the right.It will be no surprise to the reader that an extension as shown in figure 5 is straightforward.The matrix equation will contain twice as many lines as the structure contains discontinuities.

The nature of the matrix equation makes it possible to compute the field coefficients F_m and B_m at every discontinuity.Theoretically an infinite number of spatial modes m is needed to reconstruct the space- charge field at the step.Fortunately a limited number of them is sufficient to achieve a reasonable accuracy the same way that a square wave can be accurately approximated with only a few harmonic sine waves. We will come back to the problem of the required number of modes later.

3.4 The calculation of the longitudinal impedance.

In principle the response of a given cylindrical structure to a charge excitation is known in terms of electro-magnetic fields.
The longitudinal impedance is equal to the longitudinal electric field E_s integrated along the center of the structure divided by the passing current. In other words:

$$Z_{\parallel}(\omega) = (1/\rho\beta c)\int E_s(r=0,t=s/\beta c,s)ds$$

or in normal quantities:

$$Z_{\parallel}(\omega) = (a/\rho\beta c)\int E_s(p=0,t=ua/\beta c,u)du \qquad (12)$$

The integral goes from $-\infty$ to $+\infty$. Most of the fields need only be considered between consecutive steps. At the end of the structure fields exist which extend to $-\infty$ and $+\infty$. The short two step structure of figure 3 contains all the ingredients of a general structure therefore the calculation is limited to that particular case.
The waves exist in 4 types B_1,F_1,B_2,F_2, each with a given number of spatial modes. The longitudinal position of the first step is $u=0$,the second step is at $u=U$. The contribution to $Z_{\parallel}$ of mode m of wave B_1 is:

$$Z_{\parallel B_1 m}=\surd(\mu/\varepsilon_0)(a/\rho c\beta)B_{1m}z_{1m}/k_n\int(e^{j\omega t+\Gamma_{1m}u})du \tag{13}$$

It can be seen from equations (11) that C,hence,the solutions B_1,B_2,F_1 etc., contain the factor $\rho c/a$.This factor is cancelled in (13) hence from now on it is dropped altogether from the C matrix.Next,observe the presence of $\surd(\mu/\varepsilon_0)$,the 'impedance' of the vacuum,i.e. $120\pi\ \Omega$. Normalise to this impedance.Equation (13) becomes:

$$Z_{\parallel B_1 m}=B_{1m}z_{1m}/(\beta k_n)\int(e^{j\omega t+\Gamma_{1m}u})du \tag{14}$$

The same can be done for the other modes and waves.
The integral only involves the exponential propagation factor. The exponent is transformed to make it suitable for integration:

$$j\omega t+\Gamma_{1m}u=(jk_n/\beta+\Gamma_{1m})u \tag{15}$$

The integration of (14) can now be performed:

$$Z_{\parallel B_1 m}=B_{1m}z_{1m}/(\beta k_n)(jk_n+\Gamma_{1m})e^{(jk_n+\Gamma_{1m})u} \tag{16}$$

The next step is to take the integration limits into account. The 'internal' integration limits,i.e the ones determined by the longitudinal position of the discontinuity,pose no particular problem,just replace u in (16) by the corresponding normalised longitudinal step coordinate.The 'external' integration limits demand slightly more attention.These limits are at infinity. When Γ_{1m} is real then the integration result at $-\infty$ is zero.On the contrary when Γ_{1m} is imaginary then the exponent in (16) goes to $-j\infty$ defining a unit vector with arbitrary phase.Obviously we cannot proceed dragging this arbitrary phase along.It is proposed that the integration result at infinity is zero.This is a reasonable assumption for two reasons:

- suppose the integration is performed many times.Each time an arbitrary phase turns up,most probably different from preceding results.Now take the average value as the final integration result. This average is zero when a sufficient large number of trial integrations is taken.
- Also on physical grounds it can be shown that the zero result is the most likely among the possible values.The uncertainty only arises for waves that propagate in the end tubes.In our treatment this propagation occurs without losses since ohmic losses were not considered in the pipe material.To avoid the ambiguity assume that the end tubes have an infintesimally small resistivity.The infinitesimally small attenuation that will result from this is sufficient to make the fields decay to negligably small values if not to say zero at the infinite integration limits.

In the general case the expressions cannot further be simplified. The values at the integration limits have to be calculated and the results have to be summed over a certain number of modes. However when the charge is travelling with the speed of light c then $\beta=1$.An internal redundancy in the infinite sum over the modes m can be exploited under certain conditions. In the following calculation the indices $_{1,2}$ etc. are dropped.
From equations (12),(13) and (14) it follows that the impedance calculation involves an integral $\int E_s(0)du=E_s(0)/(jk_n-\Gamma)$. This integral has to be evaluated at every discontinuity and at $+\infty$ and $-\infty$.
The previous relation is transformed algebraically:

$$\int E_s(0)du = -E_s(0)[(\Gamma + jk_n)/z^2]$$
$$= -E_s(0)\Gamma/z^2 - E_s(0)jk_n/z^2 \quad (18)$$

We are interested in the first term which in our convention involves a sum at the discontinuities.The values to the left of a step carry a -sign while the the ones to the right carry a +sign. (a consequence of the integration) From the set of equations (5) the following relation can be derived :

$$\int E_r dp = E_s(0)\Gamma/z^2 \quad (19)$$

The integration is to be performed over the radius of the pipe at the step under consideration.
The field E_r is continuous at every step and also its integral over the pipe cross-section.However it must not be forgotten to take the space charge term into account.The continuity equation has to be written as an equality between integrated radial fields left and right from each step.When the structure starts and ends with the same pipe radius then the space charge contributions cancel. But then we are left with:

$$\int E_r dp_{left} = \int E_r dp_{right}$$

or in other words the first term in equation (18) is zero which introduces a considerable simplification. This is not the only benefit of this operation.The impedance for a structure can be calculated for a different number of modes.The accuracy of the computation is expected to improve as the number of modes is larger. For the case $\beta = 1$ the results do not change significantly for more than 6 modes.For $\beta < 1$ at least 12 modes are needed to achieve a similar precision.

3.5 Conclusion of this chapter.

In the preceding paragraphs it is shown that the field coefficients can be calculated in a computer for a cylindrically symmetric structure consisting of an arbitrary sequence of cross-section variations.From the knowledge of these field coefficients a value of the longitudinal field integrated along the chamber axis can be derived.In the case of ultra relativistic particles,$\beta = 1$,and for end tubes with the same radius a very good accuracy is achieved with a small number of spatial modes. The condition on the end-tube radius is not a serious constraint.Indeed, the vacuum chamber of an accelerator is closed on itself. The calculation is done for a given frequency.It can be repeated for any frequency .It is possible to make a frequency scan over an arbitrary range with any suitable resolution. All these features have been implemented in a computer program called CISLIM.

4. RESULTS OBTAINED FOR BELLOWS.

4.1 The general case

. The bellow structure of figure 6 was first analysed with the time domain analysis program TBCI . [1] The output of this program is shown in figure 7.The nature of a low Q resonator is evident but the origin of the characteristic response is not very clear.The same structure is analysed with the frequency domain program CISLIM presented in this paper.The output is shown in figure 8. The impedance as shown in figure 8 produces exactly the response shown in figure 7 when subjected to the excitation of the short bunch which was used in TBCI.The two programs give the same answer but the first one does it in the time domain,the second one in the frequency domain.In order to clarify the arguments that follow a slightly different bellows was calculated.The result is shown in figure 9. Remark the very typical repeating resonant peaks at higher frequencies. These features recall the properties of open or short circuited loss-less electrical lines.This electrical line can be identified in the bellow structure as will be shown below.

The wavelength of the resonant frequency is equal to 4 times the electrical length of the short circuited parallel line formed by an undulation.The short circuit is simply the pipe material at radius P. The mechanical length of this line is P-1.
The electrical length = P-1 + G/2
Many simulation results obtained with CISLIM have confirmed the model.
The outputs clearly indicate that the resonator is heavily damped. In other words the resonating structure looses energy via the waves in the end tubes. It is possible to calculate analytically the damping of the resonator in a very approximate way.Since it agrees well with the computer simulation results it will be repeated here.

4.1.1 Two parallel plates with a stub

The set-up is shown in figure 10.The stub is considered to be loss-less line shorted at $\lambda/4 = P-1$.The spacing between the two conductor plates is U and the distance of the two main plates at the left and the right is 2(the half distance is the normalisation factor). The extension perpendicular to the plane of the figure is l

The current of the line continues to flow in the main plates.We now imagine a common fictive return conductor for the top and bottom line. This return conductor lies in the plane of symmetry as indicated in figure 10. The fictive conductor together with the main conductor plates also form a loss-less parallel line of infinite length. This line is loading the quarter wavelength stub with its characteristic impedance. The characteristic impedance of the fictive infinite line is:

$$R_0 = 2/\pi l \qquad \text{in units of } \sqrt{(\mu/\varepsilon_0)}$$

4.1.2 The circular case.

Very bravely we replace l by 2π ,i.e.the pipe circumference,and use the same formulation as in the parallel plate case.The characteristic impedance becomes:

$$R_0 = 1/\pi^2 \tag{20}$$

This is in good agreement with the results obtained with the program for a single undulation.

4.1.3 Circular case,a sequence of undulations.

When the number of undulations is increased then the load R_0 stays the same while the total inductance increases.Hence the quality factor Q is expected to decrease.The simulations show that this actually is the case but that Q tends towards a minimum value after a relatively small number of undulations.This can tentatively be explained as follows:
The current in the equivalent plate geometry flows only in the same direction for a length in the order of $\lambda/2$.Hence a structure consisting of a large number of undulations can be split in *atomic* units of length $\lambda/2$.The quality factor of the structure will be equal to the quality factor of the $\lambda/2$ unit.

$$Q_{lim} = R_0/\omega_r L = 4/(\pi^2 ln\,[P]) \approx 4/\pi^2(P-1) \tag{21}$$

where L is the inductance of the undulations for a total length of $\lambda/2$.
For the intermediate case where the undulations occupy less than $\lambda/2$ the following relation applies:

$$Q = 4/\pi^2 \ell U \qquad \ell U < (P-1) \tag{22}$$

where ℓ is the number of undulations.
The model remains reasonably valid for $U < P-1$.For the higher resonant modes, $\ell = 2,3,...$,this condition becomes

$$U < (P-1)/(2\ell + 1)$$

The simulation indicates larger and larger damping for the higher resonant harmonics.This progression however is no longer linear in ℓ.That means that the *line picture* gradually breaks down.
Figure 11 shows the evolution of the quality factor of a bellows structure as a function of the number of undulations ℓ as derived from the computer simulation and the analytical formula.

Typical bellow geometries have P-1 = 0.2 .From formula (21) it can be seen that the quality factor Q for such a structure should be around 2 surprisingly close to the Q = 1 of the standard broadband impedance model.

4.2 A special case :the 70 Gev/c proton synchrotron in Serpukhov (SU 70)

The SU 70 machine in Serpukhov is a nice example of the material presented in the above paragraph.The vacuum chamber is corrugated over about 80 percent of its circumference.This was done to achieve sufficient mechanical rigidity for an elliptical chamber with semi-axis of 85mm*58mm.This aperture is needed to accomodate the large emittance of the injected proton beam.The undulation depth is 10 mm and the pitch 11 mm.The simulation with the equivalent circular chamber yields the following results:

$\omega_r/2\pi$	:	6.19 GHz
$\Im(Z/n)$	:	15.5 Ω
$\Re(Z/n)$	:	45 Ω
Q	:	2.9

The Serpukhov team reports in [5] on the results obtained with the direct observation of μ-wave signals.For all high energies they find a resonant frequency $\omega_r/2\pi = 5.65...6$ GHz.From threshold considerations they conclude that $\Re(Z/n) = 80\ \Omega$.However this last figure is critically dependent on the exact knowledge of the bunch length.All in all a satisfactory correspondence with the theoretical calculation.

The Serpukhov results are also interesting in another respect. Indeed the real part of Z/n was measured both at high (70 Gev/c) and low (7 Gev/c) energy.This revealed an energy dependence of the impedance.Balbekov investigated this theoretically [6]. The SU 70 structure was then also analysed with CISLIM in the mode $\beta < 1$ .A similar energy dependence was found. This is illustrated by figure 12 which gives a plot of the impedance ratio:

$$Z(\beta < 1)/Z(\beta = 1) \quad \text{or} \quad Z(\beta\gamma \ll)/Z(\beta\gamma \gg)$$

The impedance reduction is less than 10 percent for energies above 20 Gev/c.

5. CALCULATION OF THE SPS IMPEDANCE FROM VACUUM CHAMBER GEOMETRY

The SPS vacuum system contains many bellows but,as will be shown later,they are not the most contributing elements to the impedance. In fact the vacuum pump-port chamber at every magnet unit turns out to be one of the most contributing elements.Moreover it is a more complicated structure than a bellows.An example is shown in figure 13.The analysis with CISLIM is shown in figure 14 and a frequency zoom in figure 15 and 16.The value of $Z/n = 1.8\mathrm{m}\Omega$. This value is derived from the slope of the imagimary part of the calculated impedance at low frequencies,that is far from any resonance. The lowest resonance occurs at f = 1.35 GHz with an extremely high quality factor.We are far from the bellows case ! The resonant frequency corresponds with the frequency of the lowest propagation mode in the largest part of the cavity.In practice these resonances are damped by resistances which are mounted in this vacuum chamber. The program looses precision close to the resonant frequency.This is due to the fact that the impedance calculation involves sums and differences. The numbers become extremely large near a resonance and produce even unphysical negative results for $\Re(Z_{\parallel})$ as can be seen in the figures.

A bellows is imbedded in the vacuum chamber shown in figure 13. The analysis with and without this bellows gives nearly identical results.The reason for this is that the volume enclosed by the bellow undulations is negligably small with respect to the total cavity volume.No sign is found of a loaded structure so characteristic of a sequence of undulations.

This particular vacuum chamber is being modified.Indeed tungsten diaphragms are installed which will shield the nearby magnets from the synchrotron radiation emitted by circulating electrons when the SPS is used as the injector for LEP. It introduces two cross-section variations at very short distance from each other near the middle of the cavity.Also this perturbation does not alter the results obtained with the basic chamber.

5.1 Computation of the SPS impedance from the hardware

The example of figure 13 illustrates the fact that in some respects cylinders are an important ingredient in the SPS vacuum chamber system.On the other hand quite a few vacuum chambers are not round at all,e.g. the almost square vacuum chamber in the bending magnets which is the end tube for many structures of the type shown in figure 13.For the calculation this rather flat end tube has been replaced by a round one in such a way that the cut-off frequency is the same in both cases.

Following table gives an overview of the results of computer calculation of $Z_{\parallel}$ of the various type of vacuum chamber that exist in the SPS.Some remarks are necessary to clarify the information contained in table 1.
The isolated bellows are designated by their inner and outer diameter in mm.The same is true for the vacuum chamber transitions.The latter ones are calculated for two cross-section variations which are separated by many vacuum chamber diameters.The heading *Special chambers* covers a large family of different vacuum chambers. The first three are the ones which were treated in the previous paragraph.The 'ZS pot' is a chamber mounted at both ends of the electrostatic septa,while TAL,TAW and TAC are chambers of the collimator system.BBSR is the vacuum chamber of the wirescanner.The next items are the electrostatic pick-up stations,Schottky pick-up,deflectors for horizontal and vertical transverse feedback system and the vacuum chamber of the horizontal electrostatic separators. The next heading *Special magnets* concerns the vacuum chambers of magnetic septa and fast kicker magnets for injection,extraction and tune measurement. The headings *Directional couplers* and *Cavities* are self explanatory.

The values found under the column heading Z/n are calculated with the program CISLIM while $Z_{\perp}$ has been derived using the classical formula

$$Z_{\perp} = (2R/b^2)(Z/n) \tag{23}$$

where b is the radius of the continuous beam tube.For cylindrical pipes b is well defined.When the end tubes are not cylindrical,as is often the case in the SPS,an equivalent value for 'b' has to be found.H.Hereward has proposed following relation between the radius b of the equivalent cylindrical tube and the half-height h of a flat chamber:

$$b^3 = h^3/[2(\xi-\epsilon^*)] \tag{24}$$

where ξ and ϵ^* are the Lasslet coefficients for the coherent and incoherent image tune shifts.
The image coefficient ξ is zero in the horizontal plane leading to negative values for b^3 and hence for the coherent horizontal tune shift.The sign is relative in the sense that for a flat chamber the coherent tune shift caused by the wall impedance has the opposite sign of the tune shift in the vertical plane and this is the origin of the negative signs in the $Z_{\perp}$ columns of table 1.

The main contributions to the impedance come from vacuum port chambers (the first three lines of 'Special chambers'),the accelerating cavities and to a lesser extent from the special magnet cham-

Table 1: SPS impedance computed from hardware

ELEMENT	Number	b/h mm	Z/n /element mΩ	Z/n Ω	$Z_\perp$ Hor MΩ/m	$Z_\perp$ Ver MΩ/m
ISOLATED BELLOWS						
165/185	739	78.	.122	.09	.033	.033
300/340 W	154	135.	.1475	.0277	.003	.003
300/340 H	6	135.	.616	.0037	.0004	.0004
TRANSITIONS						
65/135	2	65.	3.867	.00773	.004	.004
78/109	40	78.	.994	.04	.0145	.0145
115/170	2	115.	1.911	.0038	.0006	.0006
78/170	2	78.	5.477	.011	.004	.004
78/136	24	78.	2.45	.0588	.0213	.0213
136/170	6	136.	808	.0048	.0006	.0006
SPECIAL CHAMBERS						
V.P. .75/.75	336	22.	2.886	.97	−2.77	4.4
.75/1	168	22.	2.411	.405	−1.16	1.84
1/1	486	30.	1.796	.873	−1.34	2.13
ZS Pot	10	22.5	5.387	.0539	−.15	.23
TAL/TAW	9	135.	2.283	.0205	.0025	.0025
TAC	1	78.	4.162	.0042	.0015	.0015
BBSR	3	78.	2.392	.0071	.0026	.0026
ES PU H	108	22.	.038	.0041	−.012	.019
ES PU V	108	43.	.023	.0025	.003	.003
Schot H/V	2	78.	4.322	.0087	.003	.003
Damper H	2	72.	4.156	.0083	.0035	−.0022
Damper V	2	18.	9.235	.0185	−.079	.126
Separator	6	80.	5.82	.0349	.012	−.0076
SPECIAL MAGNETS						
MST	16	85.	3.709	.0593	.018	−.011
MKP	3	30.5	57.711	.173	−.26	.409
MKA	3	27.	30.122	.09	−.171	.272
MKDH	2	28.	14.211	.0284	−.05	.08
MKDV	2	28.	17.97	.036	−.063	.1
MKE	7	16.	17.675	.1237	−.67	1.063
MKQH	1	17.	22.24	.02224	−.107	.169
MKQV	1	28.	19.368	.01936	−.034	.054
DIRECTIONAL COUPLERS						
BPCN	12	46.5	.1533	.0018	.0019	.0019
BPCS	13	110.5	.027	.00035	.0001	.0001
BPCO	5	86.5	.0923	.00046	.0001	.0001
ZKV	2	30.	7.273	.01454	.0355	.0355
CAVITIES						
Tr.Wave	198	65.	14.548	2.8805	1.4999	1.4999
St.Wave	1	78.	37.792	.0378	.0137	.0137
TOTAL				**6.2**	**−5.2**	**12.5**

bers.As was mentioned before the vacuum port chambers are damped with special resistors.The same is not true for the accelerating cavities and the special magnet chambers.Moreover the lowest resonances in these structures are well within the frequency spectrum of SPS bunches.The Z/n quoted in table 1 for these elements is derived from the low frequency inductance.In order to check whether this is acceptable an *effective impedance* is calculated according to:

$$Z_e = \int Z(\omega)h(\omega)d\omega / \int h(\omega)d\omega$$

where $h(\omega)$ is the bunch power spectrum.
The result of this calculation is shown in figure 17 for some high quality factor resonator.The resonant frequency is ω_r and the bunch length is 4τ.In the SPS $\omega_r\tau \approx 1$ for the structures with relatively low resonance frequency,hence the inductive part of the effective impedance is in very good approximation equal to the inductive part of the low frequency impedance.The effective resistive impedance remains small even near the maximum of the curve.

The effective impedance of the directional couplers was not computed.It is certainly much smaller than the value quoted in the table which anyway is extremely small.The impedance of these devices drops quickly beyond their cutt-off frequency which is at most,depending on the type,around 200 MHz.

From what preceeds it can be concluded that the SPS impedance can probably be approximated by a resonator at 1.35 GHz (the lowest resonant frequency of the vacuum port chamber) and some low quality factor determined by the damping resistors in the same chamber.The inductive part of $Z_\parallel$ and $Z_\perp$ in H and V has been computed with CISLIM.

5.2 Measurement of the SPS impedance with beam.

In what follows we report on experimental results concerning the inductive part of Z/n or $Z_\parallel$,the inductive part of $Z_\perp$ and the resistive part of Z/n.

5.2.1 Inductive part Z/n

When a bunch passes through a chamber with an inductive $Z_\parallel$ a decelarating voltage is generated by this inductance which modifies the longitudinal focussing of the beam and hence for a given emittance ,the bunch length.The derivation of Z/n from bunch lengthening measurements is given in appendix B. Table 2 shows that the results are in reasonable agreement with the results of previous paragraph.

Earlier measurements based on transfer function measurements of longitudinal quadrupole oscillations gave $10\ \Omega < Z/n < 18\ \Omega$. [3]

5.2.2 Imaginary part of $Z_\perp$

The imaginary part of $Z_\perp$ can be determined by measuring the coherent tune shift of a single bunch as a function of its intensity.These measurements were done several times in the SPS. The result is shown in figure 18 .The interpretation of these data has to be done carefully since two effects produce a linear tune shift dependence with the bunch intensity,that is to say the imaginary part of $Z_\perp$ and the direct space charge effect.The method to unfold the two contributions is explained in appendix C.The net result is that the two effects add in the vertical plane and subtract in the horizontal plane. Both effects are of the same order of magnitude such that the net effect in the H plane is very near zero.
The tune shift dependence can be read from figure 18:

Table 2: Bunch lengthening

N	τ_ℓ	A_b	V_b	V_{RF}-V_b	$\Im(Z/n)$
(10^{10})	(ns)	(eVs)	(MV)	(MV)	(Ω)
.4	1.65	.469	1.67	0.0	--
4.2	1.675	"	1.591	.0787	5.13
4.6	1.68	"	1.576	.0938	5.6
6.	1.74	"	1.41	.26	12.11
8	1.7	"	1.518	.152	5.26
8.6	1.75	"	1.386	.284	9.27

$\Im(Z/n) = 7.47\ \Omega$

horizontal $\Delta Q_H/\hat{i} \approx 0$ normalised equivalent emittance $\varepsilon_H = 50\ \mu$radm

vertical $\Delta Q_V/\hat{i} = 2.8\ 10^{-3}$ normalised emittance $\varepsilon_V = 25\ \mu$radm

where $\hat{i}$ is the peak current in the bunch.
This yields:

$$Z_{\perp V} = 13\ \mathrm{M\Omega/m}$$

$$Z_{\perp H} = -8\ \mathrm{M\Omega/m}$$

again in reasonable agreement with the calculations.

5.2.3 Beam measurement of resistive part of Z/n

From the hardware it is not possible to make definite statements about the resistive value of Z/n.Nevertheless it is interesting to derive the resisitive part of Z/n from beam measurements and check how effective the equivalent resonator is damped.The experimental results from [3] and [4] are used in what follows. It is claimed that $\Re(Z/n)$ can be derived from thresholds and growth rates of the μ-wave instability.The reason for this is explained below.
The calculation involves the comparison between an impedance vector and a stability contour or stability diagram.Figure 19 shows the form of the stability diagram associated with a reasonable bunch profile shown in the same figure.The general nature of the impedance is known,it is a resonator with a known inductance and resonant frequency while the shunt impedance or the quality factor remains to be determined.The maximum of the impedance vector occurs near the resonant frequency.This maximum in units of the shunt impedance is:

$$1/\sqrt{(1-1/4Q^2)}$$

For a large Q this value tends towards unity.For a quality factor close to one as is the case for the standard broadband model,the impedance vector is 15 percent larger than the shunt impedance. However the impedance at the maximum is 30° off pure resistive. There the required impedance for instability is larger by about the same amount than a pure resistive impedance.For vectors more than 30 °

off pure resistive the amplitude of the vector decrease rapidly and the required impedance increases.Hence the instability will occur somewhere between the absolute impedance maximum and the pure shunt impedance.If this impedance value is interpreted to be resistive then an error of around ten percent is made in the case of a Q = 1 resonator.The error becomes much smaller for higher Q values as already mentioned.

5.2.3.1 μ-wave stability measurements at 15 Gev/c

The beam stability is examined using the local Keil-Schnell criterion.The measured instability rise time is translated into a normalised rise time so that the stability diagram can be used to derive $\Re(Z/n)$.See appendix A.The results are summarised in table 3 below.

Table 3: μ-wave instability measurements at 15 Gev/c

bunch area	.15	.15	eVs
Half bunchlength	2.5	12.5	ns
rise time	∞	.25	ms
$\Re(Z/n)$	17.6	38.3	Ω

5.2.3.2 μ-wave measurements at 26 Gev/c

The bunch length was measured for various bunch intensities. These data are used in the following way to derive $\Re(Z/n)$:

The bunch is supposed to blow up until it is stable with respect to the μ-wave instability.The stability criterion involves the knowledge of dp/p,the corresponding half bunch length τ_ℓ which together determine the bunch area A_b and finally a factor derived from the stability diagram (local application of Keil-Schnell criterion).In order that a longitudinal stability is efficient its rise time needs to be shorter than the synchrotron period.Since the beam is at the treshhold of instability the rise time is taken equal to the synchrotron period.This in turn determines a normalised rise time in terms of the resonant frequency of the resonator (1.35 GHz) and the amplitude of the impedance vector in the stability diagram which is just stable.See also appendix A.This then determines completely the stability criterion and allows the computation of $\Re(Z/n)$.The summary is in the following table 4

5.3 Conclusion

The inductive impedances derived from beam measurements in the SPS are in extremely good agreement with the values derived from the hardware using the computer code presented in this paper. The total equivalent impedance of the SPS is a broadband resonator with a quality factor of around 6.This is based on the value of the shunt impedance calculated with the results on the μ-wave instability.The agreement with the accepted model of a Q = 1 resonator is fair.

Table 4: μ-wave instability measurements at 26 Gev/c

N	τ_ℓ	$\Re(Z/n)$
10^{10}	ns	Ω
10.5	1.775	41.8
10	1.81	45.2
12	1.86	41.8
12.8	1.86	38.3
13	1.925	41.8
14	1.96	38.3
15	2.01	38.3
16.6	2.1	34.8

$$<\Re(Z/n)> = 40\ \Omega$$

Acknowledgments

It is a pleasure to thank J.Gareyte for the very carefull proofreading of the report and for his support throughout the preparation.

APPENDIX A

APPLICATION OF LOCAL KEIL-SCHNELL CRITERION TO BUNCHES

It has been proposed by D.Boussard [7] that the Keil-Schnell criterion for the stability of DC beams can be used locally in order to examine the stability of bunches against very high frequency (μ-wave) instabilities.This makes it possible to use a dispersion analysis to establish thresholds.
The stability condition for DC beams can be written in the following form (see also [8]):

$$(Z/n)(Ne/T)/(dp/p)^2 = 2\pi(E/e)\beta^2|\eta|jd(\xi)^{-1} \qquad \text{(A-1)}$$

where T is the revolution period,E the beam energy,N the number of particles and $d(\xi)$ the inverse stability contour for a normalised frequency ξ. The longitudinal stability criterion is characterised by the derivative of the particle distribution function.This makes it difficult to use a pure parabolic distribution since it would be perfectly unstable all the time.Therefore a parabolic profile with smoothed edges was adopted.

Formula (A-1) has now to be adapted to the case of a bunched beam.First the number of particles N becomes the number of particles in a bunch.Next it is the local intensity that counts and not the average intensity.Hence T is replaced by $2\tau_\ell$ where τ_ℓ is the half bunch length.A final modification concerns the value for $1/d(\xi)$.A DC beam is unstable when the instability rise time exceeds zero. This corresponds to a well defined contour in the stability diagram.For the example of a parabolic distribution with smooth edges $1/d(\xi) \approx 1/5$.
The instability rise time for a bunched beam needs to be shorter than a synchrotron period in order to be efficient. The correction is small for the μ-wave instability in the SPS. Indeed the synchrotron frequency is small with respect to the longitudinal frequency spread at 1.35 GHz.The stability margin is only reduced by about 10 percent.

APPENDIX B

CALCULATION OF INDUCTIVE WALL FROM BUNCH LENGTH MEASUREMENT

The equation of the longitudinal motion in the absence of a wall impedance can be written in the following form:

$$d[(E/h\eta\Omega^2)(d\phi/dt)]/dt - e\hat{V}(\sin\phi - \sin\phi_0)/2\pi = 0$$

where $\hat{V}$ is the amplitude of the RF voltage, ϕ the phase between the particle and the RF wave and Ω is angular revolution frequency. The other symbols have their usual meaning.
When the motion is linearized then the second term is modified:

$$e\hat{V}(\sin\phi - \sin\phi_0)/2\pi = (e/2\pi)\Delta V = (e/2\pi) < dV/d\phi > \Delta\phi \quad \text{(B-1)}$$

The average voltage gradient $< dV/d\phi >$ can be easily calculated for stable phase angle $\phi_0 = 0$:

$$< dV/d\phi > = (\hat{V}/\phi_\ell)\,{}_0\!\int^{\phi_\ell}\cos\phi\, d\phi = \hat{V}\sin\phi_\ell/\phi_\ell$$

where ϕ_ℓ is the extreme RF phase of the synchrotron orbit that is considered.
Equation (B-1) becomes:

$$(e\hat{V}/2\pi)\sin\phi = (e/2\pi)\hat{V}(\sin\phi_\ell/\phi_\ell)\Delta\phi \quad \text{(B-2)}$$

The presence of an inductive wall impedance will modify the longitudinal focussing. The inductance and Z/n are related as follows:

$$L = \Im(Z/n)/\Omega$$

The voltage induced by a passing bunch will be:

$$V_L = L(di/dt)$$

The current of a parabolic bunch is:

$$i = (3/4)(Ne/\tau_\ell)[1-(t/\tau_\ell)^2]$$

Hence the induced voltage takes the form:

$$V_L = -(3/2)(Ne/h\Omega^2\tau_\ell^3)(Z/n)\Delta\phi \quad \text{(B-3)}$$

where the substitution $\Delta\phi = h\Omega t$ was used.
The gradient of the induced voltage is constant over the bunch length.

$$dV_L/d\phi = -(3/2)(Ne/h\Omega^2\tau_\ell^3)(Z/n) \quad \text{(B-4)}$$

The modified equation of motion can be rewritten using (B-2) and (B-4):

$$d[(E/h\eta\Omega^2)(d\phi/dt)]/dt - (e/2\pi)(\sinh\Omega\tau_\ell/h\Omega\tau_\ell)(\hat{V} - (3/2)Ne/(\Omega\tau_\ell^2\sinh\Omega\tau_\ell)Z/n)\Delta\phi = 0$$

The equivalent RF voltage reduction caused by the inductance is

$$\Delta\hat{V} = -(3/2)Ne/(\Omega\tau_\ell^2\sinh\Omega\tau_\ell)Z/n$$

This expression fits the usual formula for small $\Omega\tau_\ell$ and yields a value for the inductive part of Z/n:

$$\Im(Z/n) = -(2/3)(\Omega\tau_\ell{}^2 \sinh\Omega\tau_\ell/Ne)\Delta\hat{V} \tag{B-5}$$

The measurement of $\Im(Z/n)$ can now proceed as follows:
The half bunch length τ_ℓ and the number of particles N in the bunch are measured.The external RF voltage $\hat{V}$ is known and held constant.For sufficiently low values for N there is no voltage contribution from the inductive wall,hence the bunch area can be determined. It becomes then possible to calculate the inductive voltage reduction for the higher bunch intensities assuming that the bunch area remains constant.This is reasonable when the intensity reductions are obtained by transverse scraping.

APPENDIX C

CALCULATION OF $Z_\perp$ FROM THE COHERENT TRANSVERSE TUNE SHIFT

When a bunch is kicked transversely its oscillation frequency or transverse tune is a function of its intensity.The difference with the zero intensity tune is called the coherent tune shift. This shift is made up of two contributions:

- A tune shift caused by the space charge
- A tune shift caused by the transverse impedance $Z_\perp$

These two contributions will be examined in the case of the SPS and it will be shown how a value for $Z_\perp$ can be derived from a measurement of the total coherent tune shift as a function of intensity.

C.1 Coherent tune shift from space charge

The space charge tune shift varies along the bunch in azimuthal direction.The maximum value occurs in the center of the bunch where the charge density is largest.This maximum is:

$$\Delta Q_{sc} = (-4r_p R\hat{i}\varepsilon_0^*)/ec\gamma^2\varepsilon$$

where	$r_p = e/4\pi\varepsilon_0(E_0/e)$	classical proton radius
	ε_0^*	space charge parameter
	ε_0	dielectric constant in free space
	ε	normalised emittance
	$\hat{i}$	maximum instantaneous bunch current

This can be transformed into:

$$\Delta Q_{sc} = -\sqrt{(\mu/\varepsilon_0)}R\hat{i}\varepsilon_0^*/[\pi(E_0/e)\gamma^2\varepsilon]$$

To find a contribution to a coherent tune shift the average over the ensemble has to be found.

$$(\Delta Q_{sc})_{coherent} = \langle\Delta Q_{sc}\rangle = \int\Delta Q_{sc} f(t/\tau_\ell)d(t/\tau_\ell)$$

where $n = \int F(t/\tau_\ell)d(t/\tau_\ell) = \int F(\xi)d\xi$ particles in a bunch

$\xi = t/\tau_\ell$

$f(\xi) = F(\xi)/n = 0.75(1-\xi^2)$ for a parabolic profile

Hence $\langle\Delta Q_{sc}\rangle = 0.75\int\Delta Q_{sc}(1-\xi^2)d\xi$

But $\Delta Q_{sc} = 0.75\Delta\hat{Q}_{sc}(1-\xi^2)$

so $\langle\Delta Q_{sc}\rangle = (9/16)\Delta\hat{Q}_{sc}\int(1-\xi^2)d\xi = (3/5)\Delta\hat{Q}_{sc}$

and finally:

$$\langle\Delta Q_{sc}\rangle = -(3/5)\sqrt{(\mu/\varepsilon_0)}R\varepsilon_0^*\hat{i}/[\pi(E_0/e)\gamma^2\varepsilon] \qquad \text{(C-1)}$$

C.2 Coherent tune shift from $Z_\perp$

The inductive part of $Z_\perp$ produces a coherent tune shift for a bunch with an average intensity $<i>$ defined over its bunch length. This tune shift can be written as follows:

$$\Delta Q_c = -\Im(Z_\perp) <i> R/[4\pi\gamma(E_0/e)Q]$$

Remark that: $<i> = (2/3)\hat{i}$

The expression for the coherent tune shift caused by $\Im(Z_\perp)$ becomes:

$$\Delta Q_c = -\Im(Z_\perp)\hat{i}R/[6\pi\gamma(E_0/e)Q] \qquad \text{(C-2)}$$

C.3 The total coherent tune shift

Adding the result of the two previous sections (C-1) and (C-2), following expression is obtained for the total coherent tune of a bunch

$$\Delta Q_{coh} = -[(R/Q)\hat{i}/6\pi\gamma(E_0/e)][3.6Q\varepsilon_0{}^{*}\sqrt{(\mu/\varepsilon_0)}/(\gamma\varepsilon) + \Im(Z_\perp)]$$

It is now assumed that the contribution from the space charge can be computed accurately.That is to say that the emittances are known from which the space charge coefficients $\varepsilon_0{}^{*}$ can be calculated.
It should be noted that the formula for the total tune shift was derived for positive values of $\Im(Z_\perp)$.In that case the two terms in the expression add.For the SPS this is valid in the vertical plane.In the horizontal plane however it is expected that the two contributions subtract since a negative value for $Z_\perp$ was found in that plane.This indeed is borne out by the experiment.

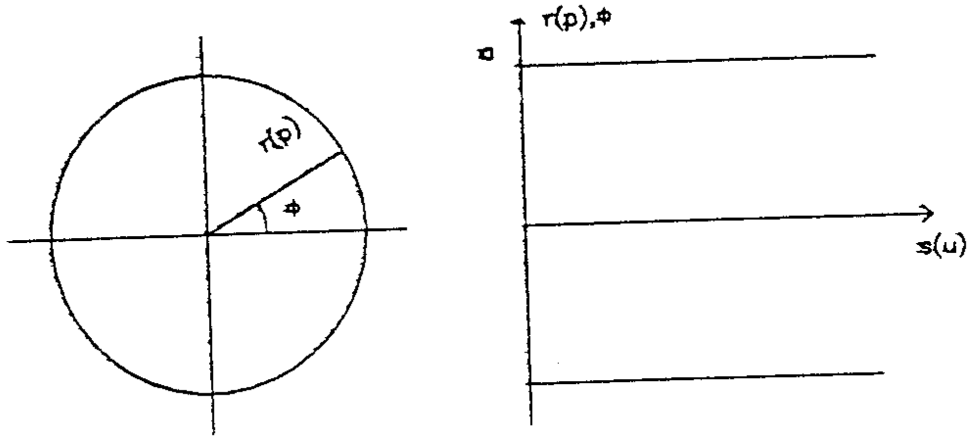

Coordinate system

FIG 1

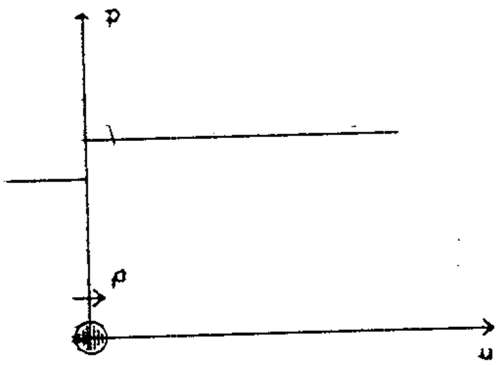

Charge passing in a pipe
with one transition

FIG 2

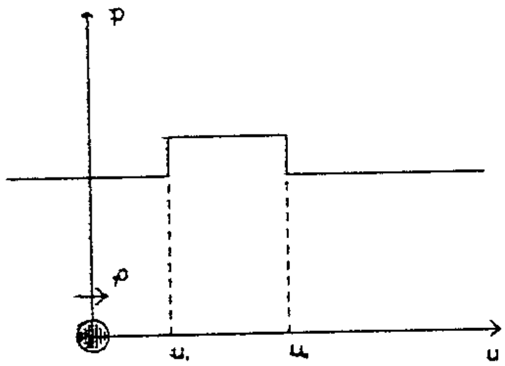

Charge passing in a pipe
with two transitions

FIG 3

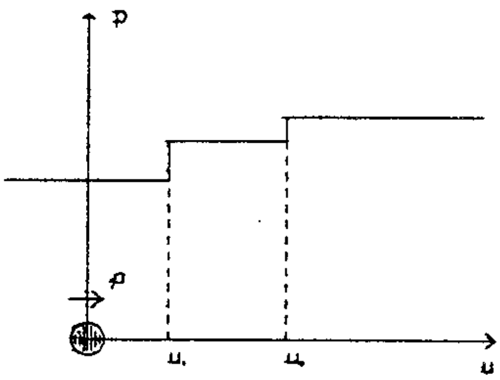

FIG 4

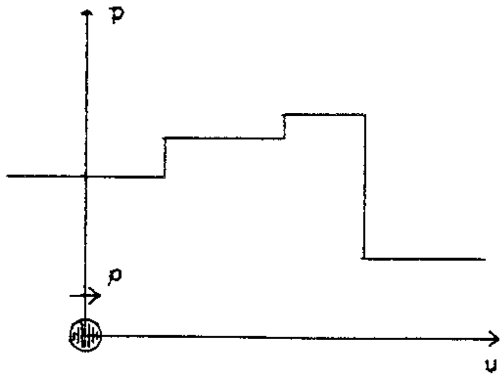

FIG 5

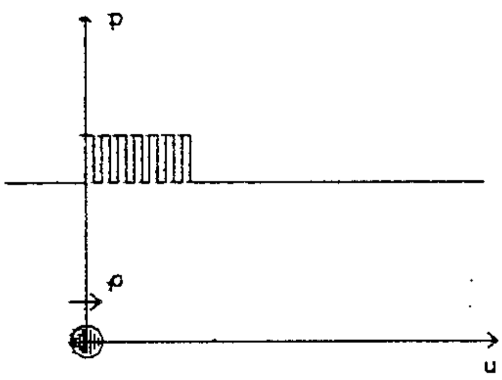

Bellows structure

FIG 6

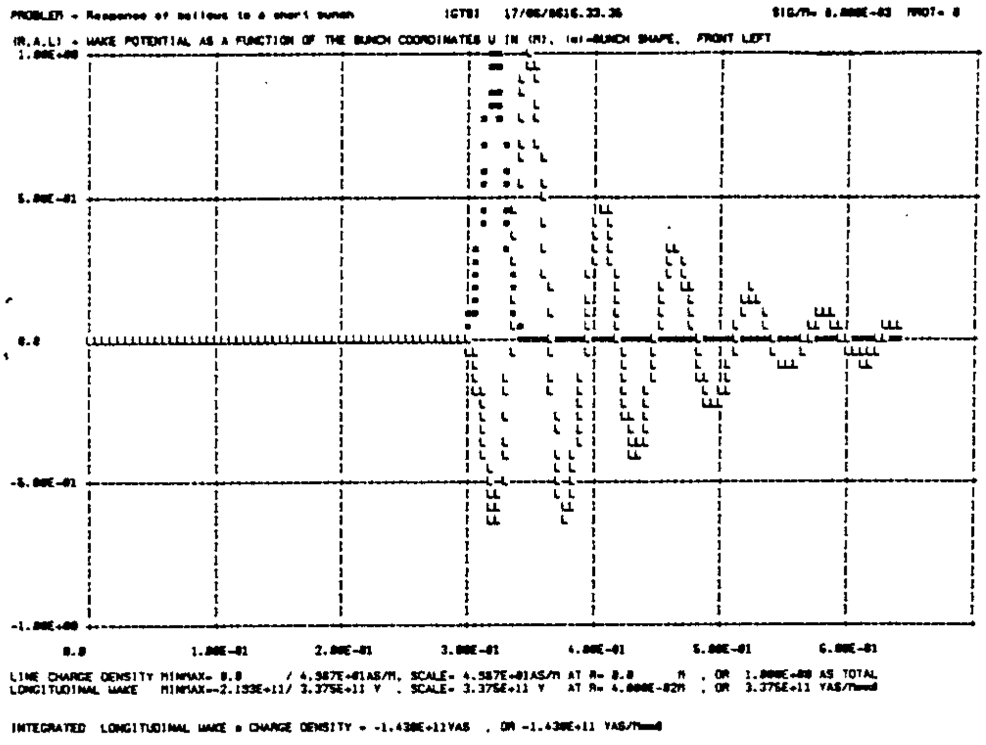

Response of bellows calculated with TBCI

FIG 7

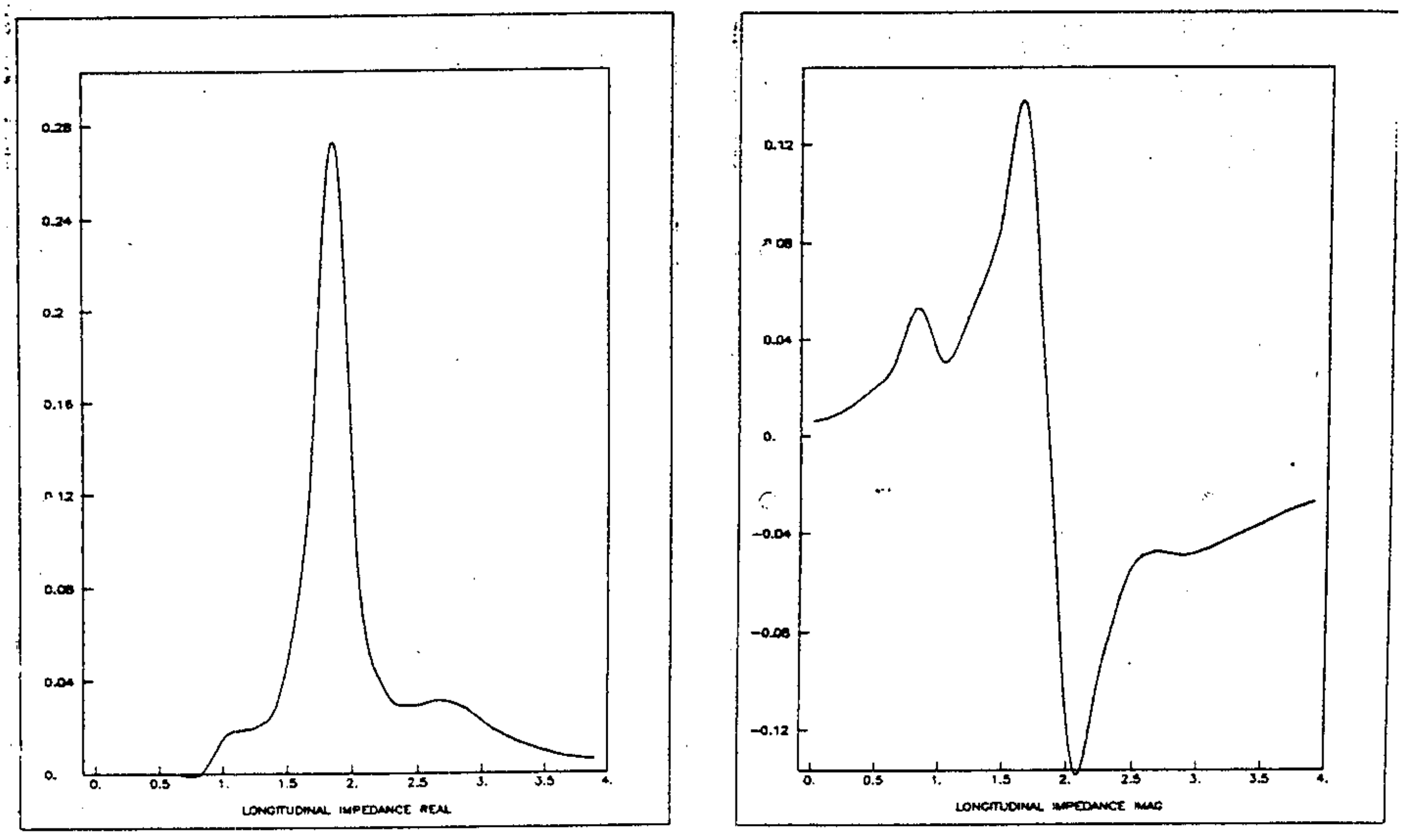

Impedance of bellows calculated with CISLIM

FIG 8

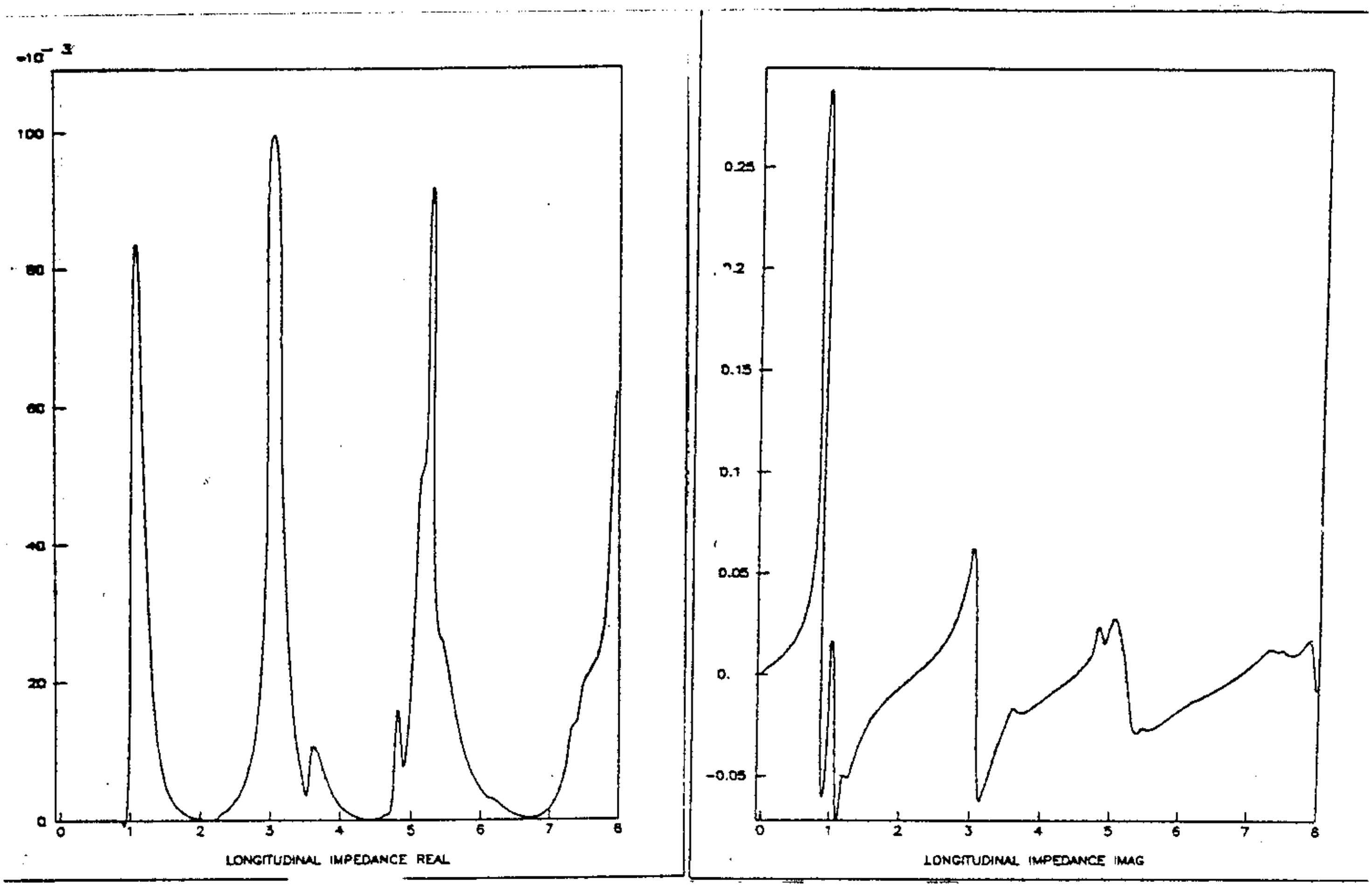

Impedance of bellows calculated with CISLIM

FIG 9

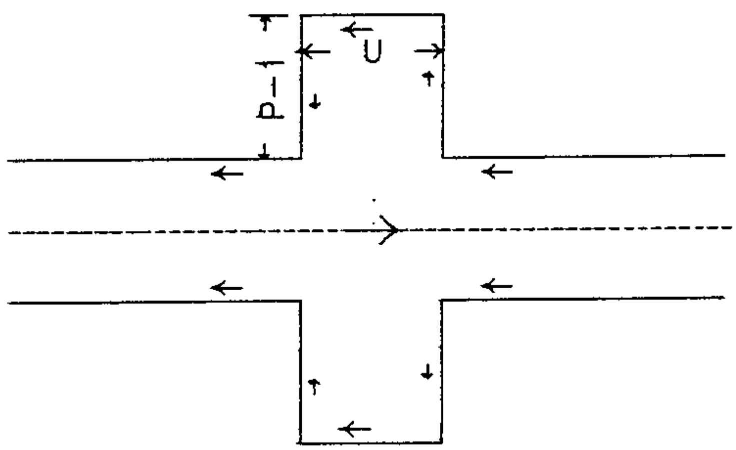

Two parallel plates with stub

FIG 10

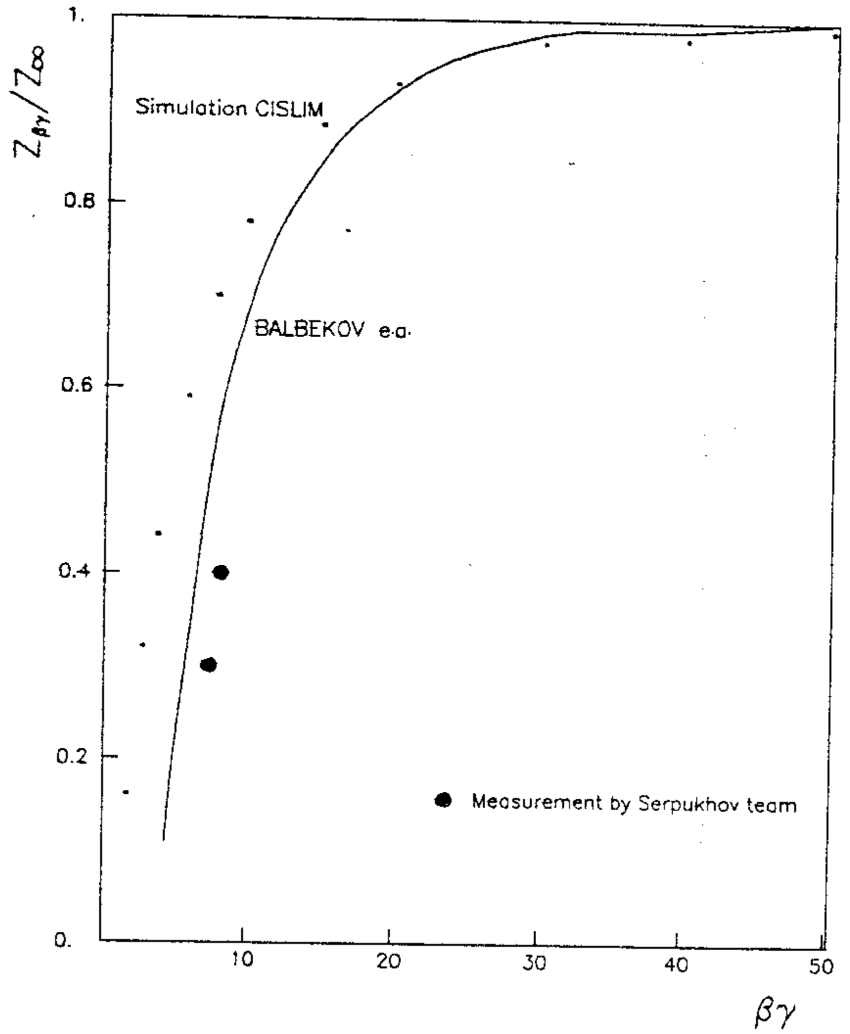

Impedance dependance on $\beta\gamma$

FIG 12

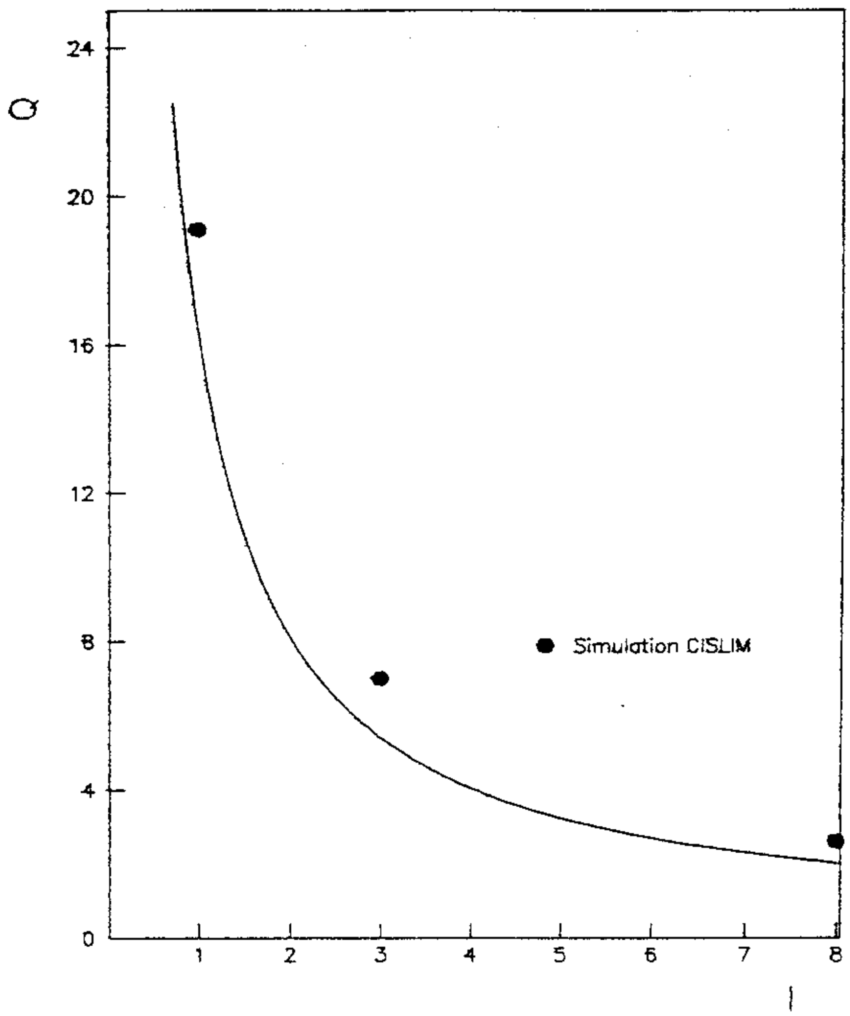

Quality factor Q versus number of undulations l

FIG 11

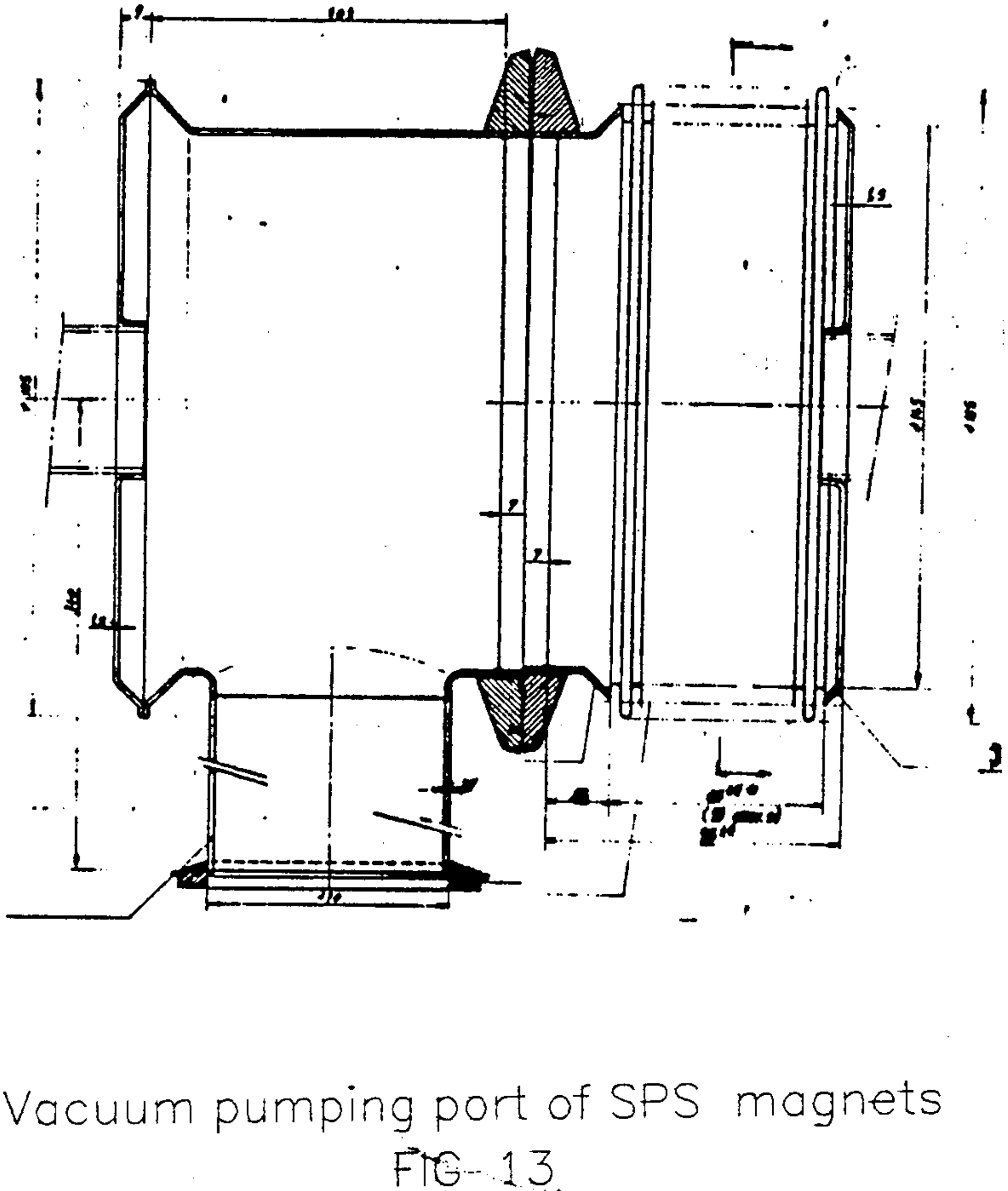

Vacuum pumping port of SPS magnets

FIG. 13

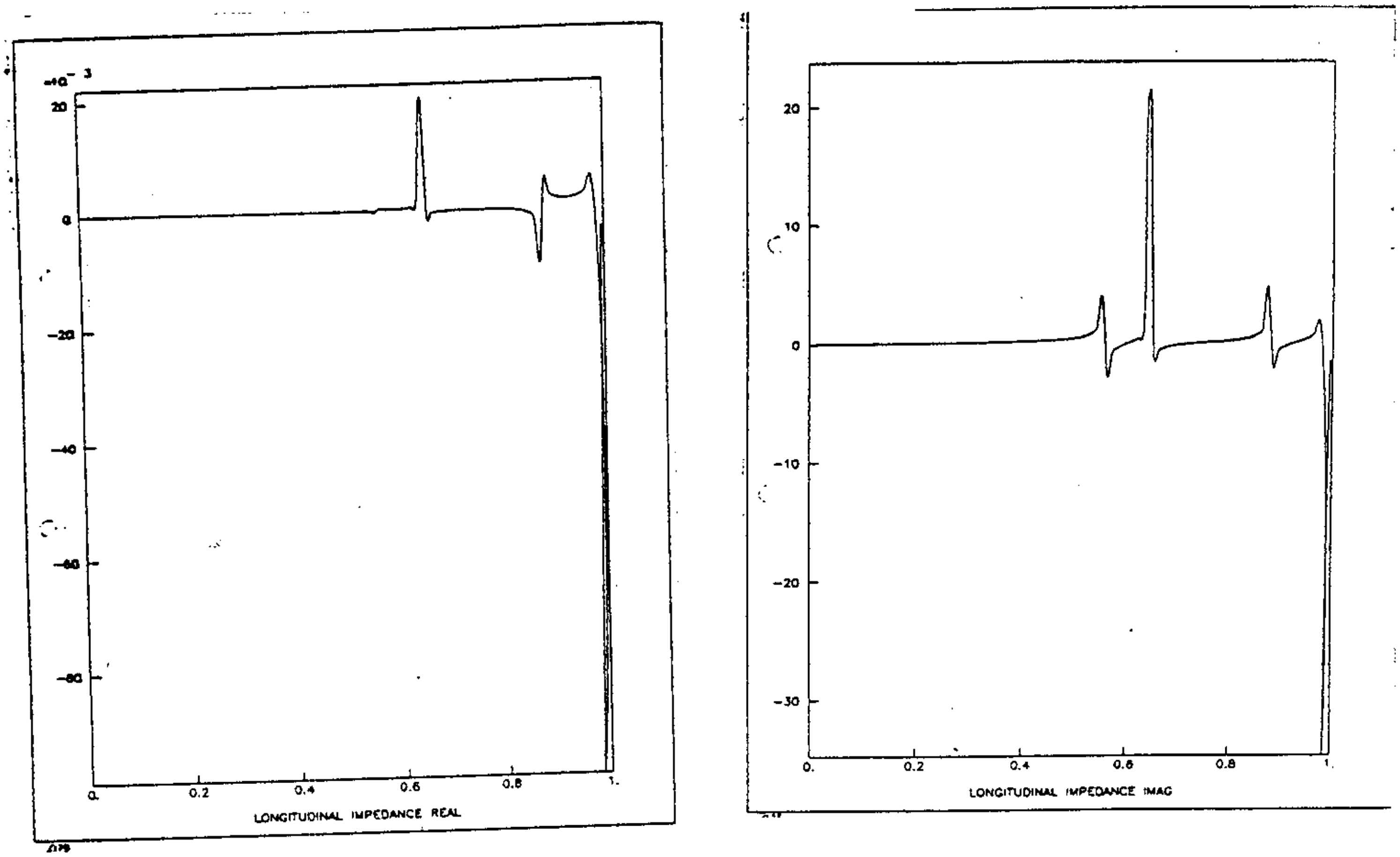

Impedance of vacuum pumping port

FIG 14

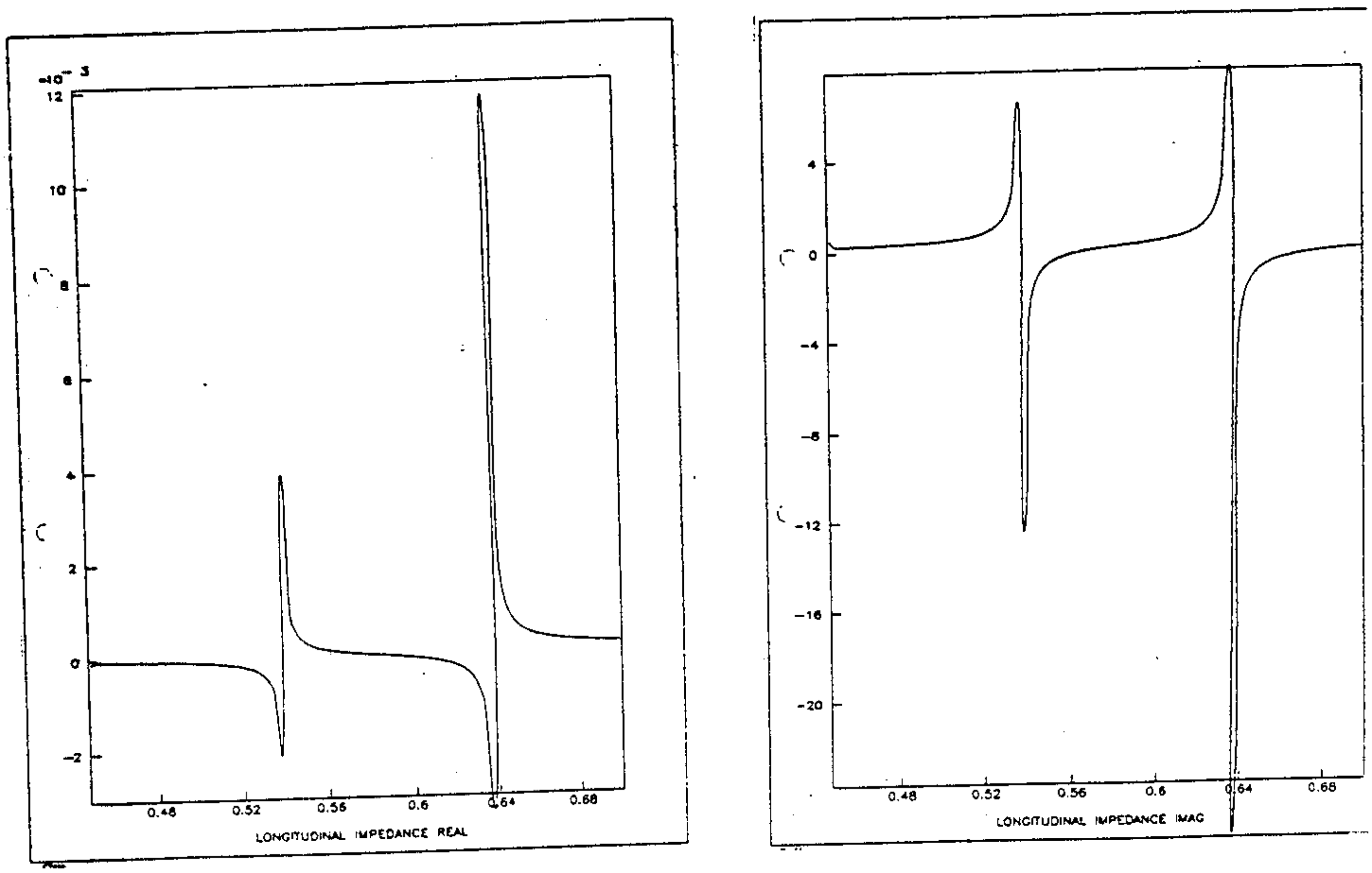

Detail of impedance

FIG 15

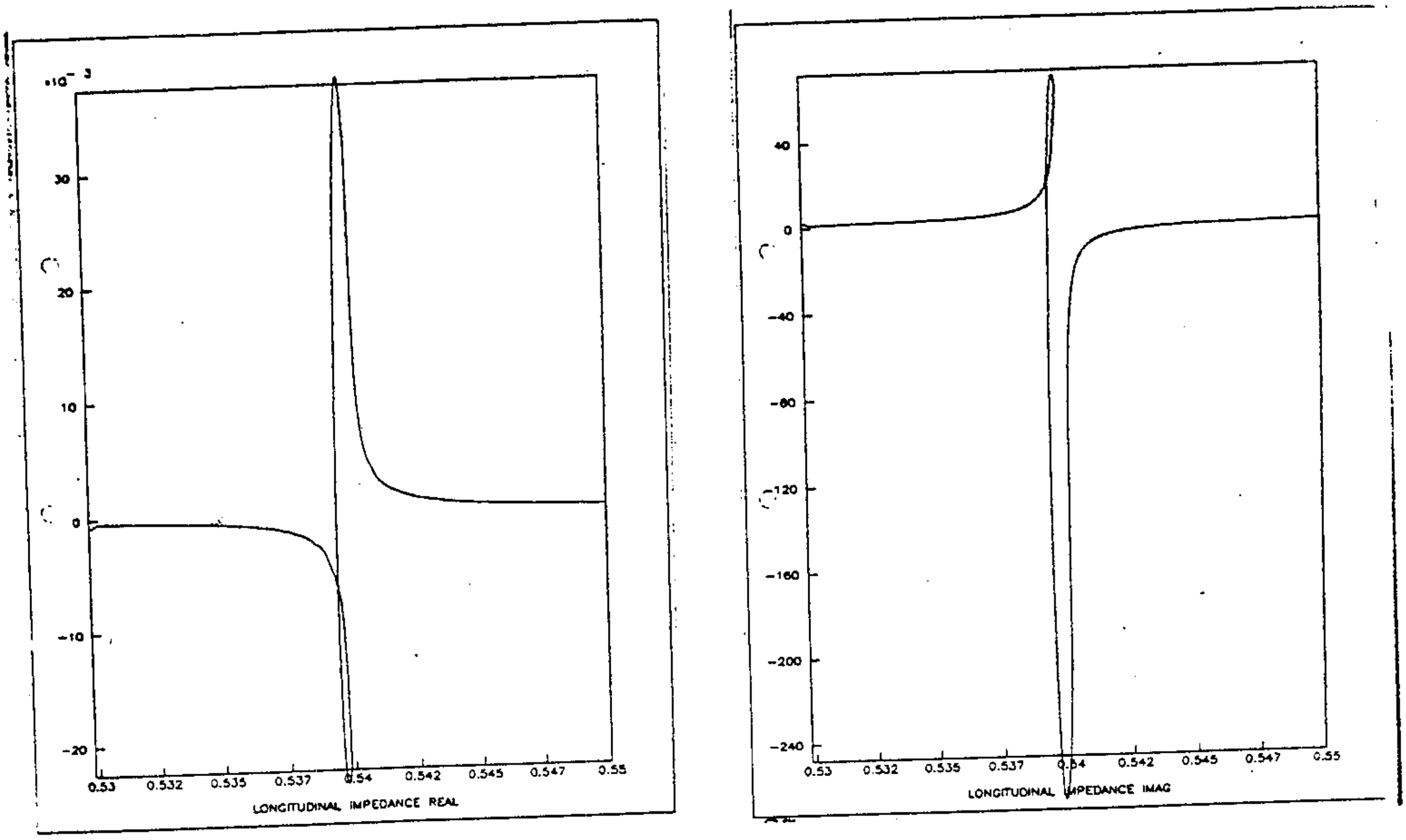

Detail of impedance
FIG 16

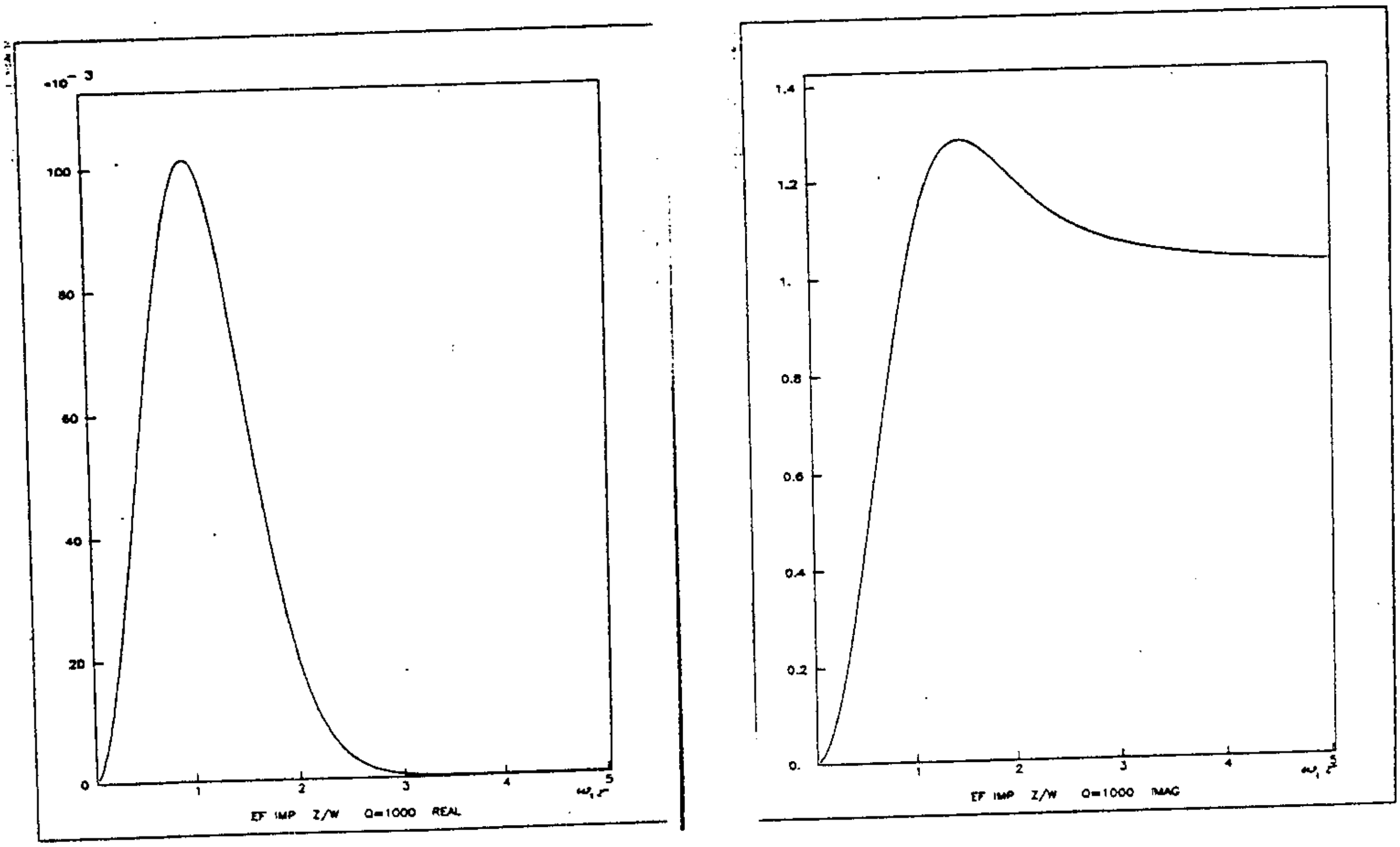

Effective impedance of high Q resonator
FIG 17

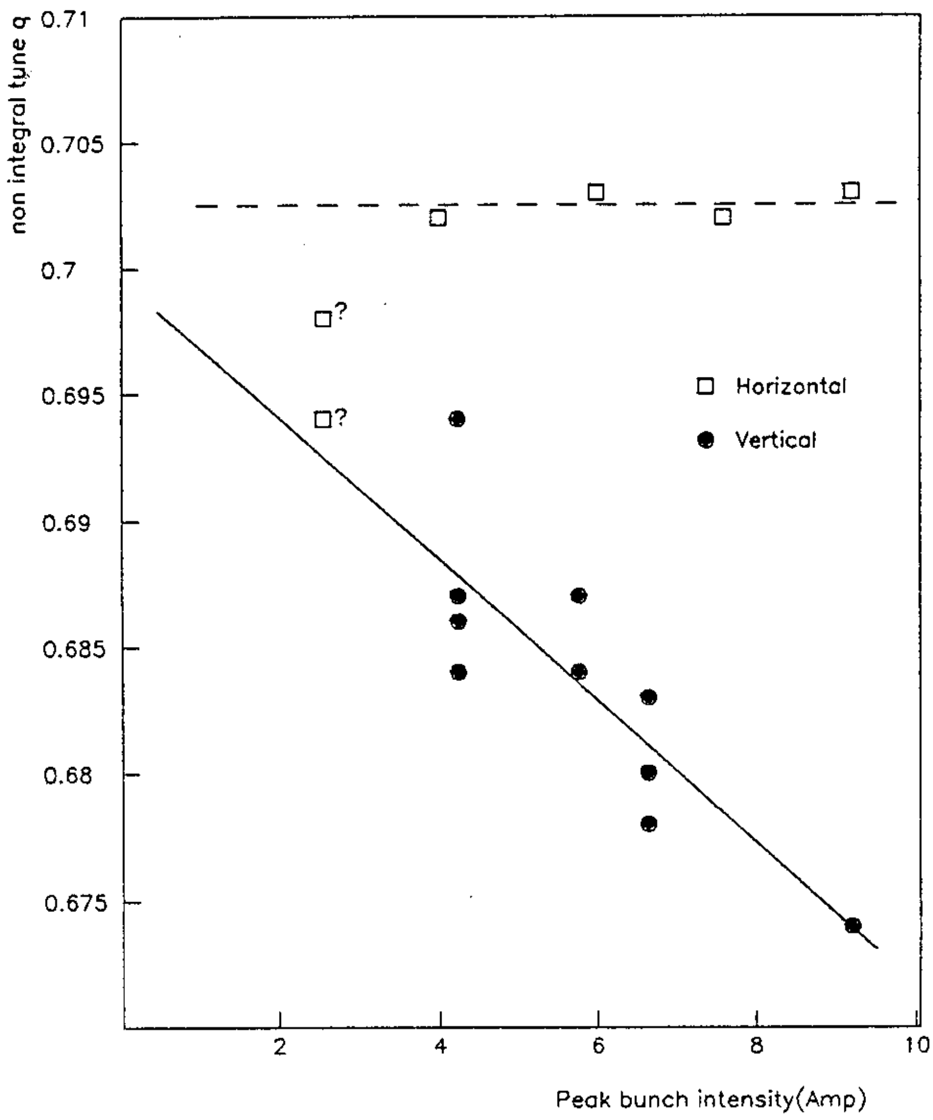

Coherent transverse tune versus bunch intensity
FIG 18

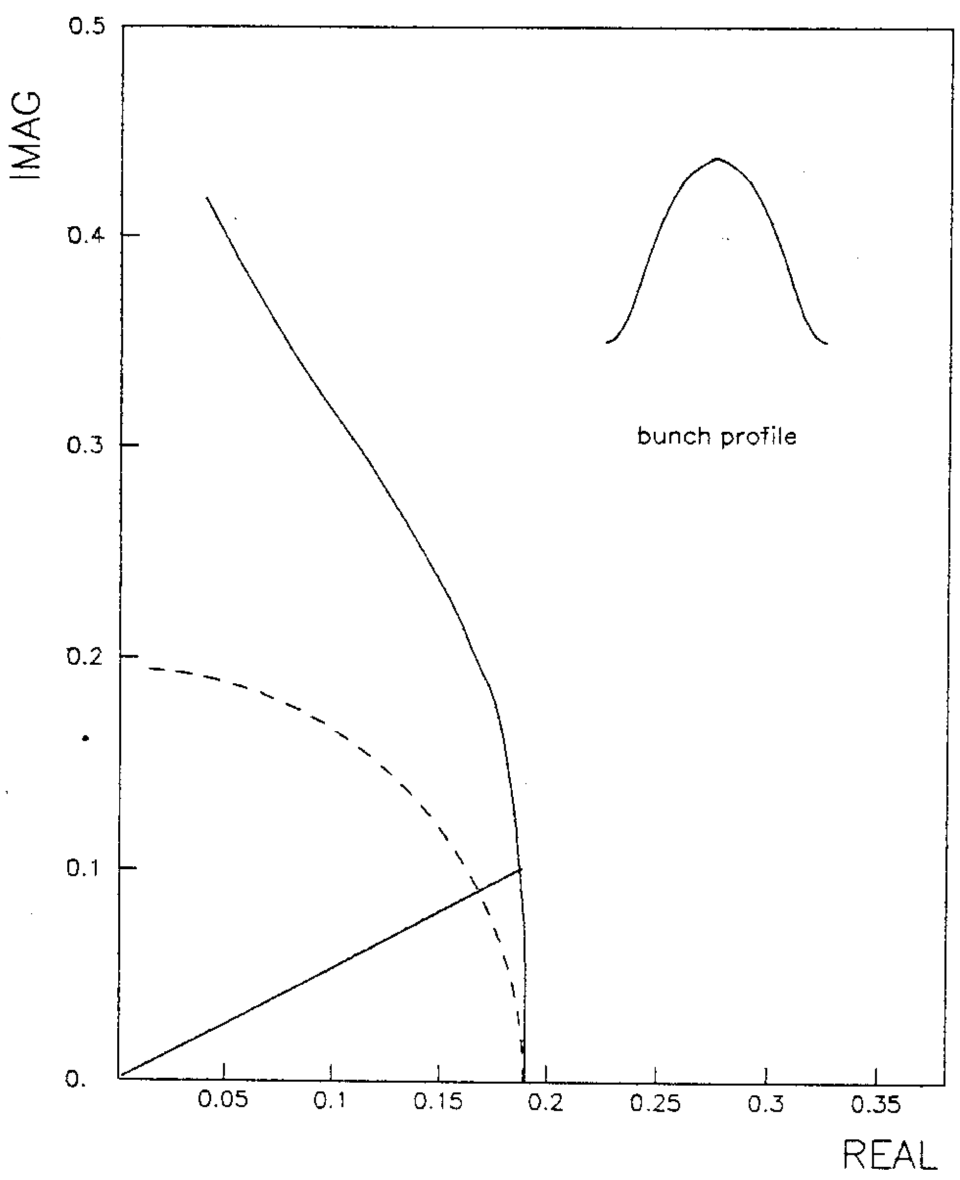

Stability diagram
FIG 19